Ir. J. van Leeuwen and A. C. van Riel

ULTIMATE-LOAD DESIGN OF AXIALLY AND ECCENTRICALLY COMPRESSED STRUCTURAL MEMBERS

U.D.C. 624.075.2

In Holland a new Code of Practice for reinforced concrete was introduced last year (designated as G.B.V. 1962).
Under the new Code, structural members subjected to axial and to eccentric compression should be designed by the ultimate-load method. The principles and practical rules of this method are set forth in Clauses 47 en 48. The theoretical considerations, verified by experimental results, on which these two clauses are based are likely to be of interest to foreign readers also, and it therefore appeared appropriate to devote an article to the subject.
In conjunction with the introduction of the new Code of Practice the notation employed was brought into line with the recommendations of the Comité Européen du Béton (C.E.B.). This notation has also been adopted in the present article.

0 Introduction

In Clause 47 of the Netherlands Standard Code of Practice for Reinforced Concrete (G.B.V. 1962) it is laid down that the ultimate-load method should be used for the design of axially and eccentrically compressed structural members. This method has been adopted because a number of objections had arisen against the conventional design method (based on the modular ratio of steel and concrete) as envisaged in the earlier Code (G.B.V. 1950). Thus, the conventional method took no account of the fact that a member subjected to bending in conjunction with direct force will deflect under the influence of the loading, with the result that the bending moment will increase. The increase will in turn produce a greater deflection, etc. This process, which is affected also by the creep of the concrete, will continue until a state of equilibrium is reached or until failure of the member occurs. The amount of deflection depends, inter alia, upon the slenderness of the member. In the conventional design method the effect of the slenderness is not sufficiently taken into account, as is, for example, apparent from tests performed by Gaede on columns provided with hinged ends and having a length/width ratio (l_c/h_t) of approx. 30. The columns were subjected to a constant eccentric compressive force for more or less long periods of time. The ultimate load (failure load) was found to be only about two-thirds of the permissible load calculated in accordance with the German regulations. A similar tendency was ascertained in tests carried out on reduced-scale slender columns by the T.N.O. Institute for Building Materials and Structures (I.B.B.C.). In actual practice, however, the boundary conditions are often likely to be more favourable. For this reason, in accordance with the French regulations and a recommendation of the Comité Euro-

péen du Béton (C.E.B.), in Clause 47 of G.B.V. 1962 the effective lengths have been made dependent upon the boundary conditions.

In buildings the theoretical height (length) of the member (l_t) is the distance measured from top of floor to top of next floor. The effective length (l_c) which enters into the stability analysis is equal to l_t in the following cases:
if the member is hinged at both ends;
or if it is restrained (*i.e.*, fixed or encastré) at both ends but one end is nevertheless free to undergo displacement in the plane of bending in a direction perpendicular to the longitudinal axis of the column.

The other cases indicated are:
$l_c = 2l_t$ for a member restrained at one end and free at the other;
$l_c = 0.7l_t$ for a member restrained at one end and hinged at the other; this value may also be adopted if – in a framed rigid-jointed structure, for example – the column is rigidly connected to the foundation or to beams having a moment of inertia at least equal to that of the column and which are furthermore rigidly secured by other structural connections;
$l_c = 0.9l_t$ should be adopted in other cases.

As the conventional design method takes no account of the non-linearity of the relation between the load, on the one hand, and the deformations and stresses on the other, the consequences of continually increasing the permissible stresses cannot be assessed with this method, even if we maintain a constant ratio between the permissible stress in a material and the strength of that material. And this inability to assess the consequences is all the greater because the computational quantities occurring in the conventional method are not measurable, so that experimental verification is very difficult or impossible.

Finally, it is known that the use of high-tensile steel with the conventional method is advantageous only if the eccentricity of the load is large. With better means of tackling the problem and deeper insight into the nature thereof it will also become possible to judge more reliably the merits of using steels of that kind.

The above-mentioned drawbacks have also made themselves felt in other countries and within the C.E.B., and attention has accordingly been directed to the adoption of the method which allows of relatively simple experimental verification: the ultimate-load method. With this method it is endeavoured to predict the ultimate load (failure load) of a member as accurately as possible, starting from the rules of mechanics, a few simple assumptions, and the available knowledge regarding the mechanical properties of the materials concerned. The permissible load is then quite simply determined by introducing a factor of safety (or "load factor"). In the present article this line of thought will be further explained. By "ultimate load" of an axially or eccentrically compressed structural member is to be understood that constant compressive

force which the member is still just able to resist for an indefinite length of time.

In the treatment of the subject the following variables will be introduced:

a. the eccentricity of the load;
b. the dimensions and shape of the member in cross-section;
c. the slenderness ratio;
d. the amount of reinforcement (also asymmetrical reinforcement);
e. the concrete cover to the reinforcement;
f. the steel quality;
g. the concrete quality.

The member is conceived as being provided with hinged connections at both ends. The treatment of the problem relates to the case where the eccentricity of the load is constant over the entire length of the member. Indications for carrying out the analysis in the case of varying eccentricity are given, however. Finally, the centre of compression is assumed to be located on an axis of symmetry of the cross-section (so-called simple bending).

1 General analysis

1.1 Ultimate load of an eccentrically compressed member

1.1.1 Principles

The analysis is based on the following principles:

a. the tensile stresses are resisted by the steel only;
b. the tensile and compressive strains of the fibres due to bending are directly proportional to their distance from the neutral axis;
c. the relation between the steel stress σ_a' (σ_a) and the strain ε_a'(ε_a) is, for simplicity, diagrammatically represented by two straight lines, as indicated in Fig. 1a; modulus of elasticity $E_a = 2.1 \times 10^6$ kg/cm^2;
d. the relation between the concrete compressive stress σ_b' and the strain ε_b' conforms to a quadratic parabola whose apex corresponds to a maximum concrete compressive strain $\varepsilon_u' = 3.5^0/_{00}$ (see Fig. 1b). This assumption is the same as that adopted at the 3rd C.E.B. Congress at Madrid in 1956. Since in tests with loading of short duration the maximum compressive strain of the concrete is generally less than $3.5^0/_{00}$ (*viz.*, approx. $2^0/_{00}$), it is assumed that the effect of the creep of concrete is taken into account in the stress-strain diagram adopted by the C.E.B. The ultimate compressive stress σ_u' is taken as 0.6 times the cube strength at 28 days. The magnitude of this factor is based on the following considerations:

   1. In the actual structure the quality of the concrete will be more truly represented by the prism strength or the cylinder strength than by the cube strength. On the basis of ample information given in the literature it may be assumed that: prism strength $\approx$ cylinder strength $\approx 0.85 \times$ cube strength.

Fig. 1a. Assumed stress-strain diagram for steel ($E_a = 2.1 \times 10^6$ kg/cm^2).

Fig. 1b. Assumed stress-strain diagram for concrete = quadratic parabola:

$$\sigma_b' = \sigma_u' \frac{\varepsilon_b'}{\varepsilon_u'} \left(2 - \frac{\varepsilon_b'}{\varepsilon_u'}\right)$$

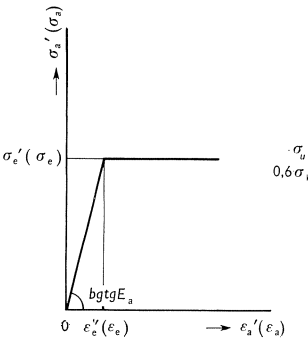

Fig. 1a.

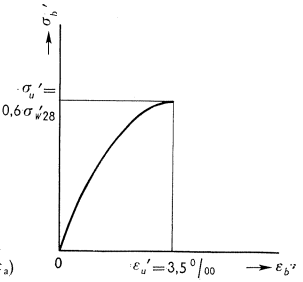

Fig. 1b.

2. It is known that, on the one hand, the compressive strength is somewhat *reduced* by the effect of a sustained or a varying load, but that, on the other hand, the strength *increases* in consequence of continued hardening of the concrete. In general, in the literature a value of between 0.8 and 1.0 is indicated for the reduction coefficient for taking account of the effect of sustained loading. In the present case a value of 0.9 has been adopted.

3. The quality of concrete cast in situ will show a certain dispersion or scatter. In the U.S.A., for example, starting from a normal distribution, a coefficient of variation (cv) of 10–15% (average 12.5%) is taken to indicate good workmanship and a coefficient of variation of 15–20% (average 17.5%) is taken to indicate moderately good workmanship. Furthermore, again starting from a normal distribution and a given value of the coefficient of variation, it is possible to determine a compressive strength $\bar{\sigma}$ as a function of the average compressive strength σ_m below which the strength is likely to fall with a given probability. Thus, for example, for 5% probability of falling short of this value:

$$\frac{\bar{\sigma}}{\sigma_m} = 1 - 1.64 \text{ cv}$$

and for 10% probability:

$$\frac{\bar{\sigma}}{\sigma_m} = 1 - 1.28 \text{ cv}$$

For a coefficient of variation of 15% the reduction factor associated with the 5% and 10% short-fall probability is 0.754 and 0.808 respectively.

On multiplying this factor by the factors indicated under points 1 and 2, we obtain, for the above-mentioned short-fall probabilities, the respective values 0.576 and 0.618 for the ratio between the guaranteed ultimate compressive strength σ_u' and the average cube strength $\sigma_{w_{28}}'$. In the Dutch

regulations a value of 0.60 has therefore been adopted as a reasonable average.

e. A sinusoidal shape has been adopted for the deflection curve of an eccentrically loaded member with hinged ends. From GAEDE's tests and tests performed by the I.B.B.C. it appears that this shape is within the accuracy of measurement, even in the cracked range.

1.1.2 Equilibrium conditions

When a load on a structural member is increased, the conditions of equilibrium should continue to be satisfied right up to the instant of failure. Fig. 2 indicates a state of strain associated with a compressive force N' acting eccentrically upon a rectangular section. The state of strain is determined by certain values ε_1 and ε_2 at the two extreme fibres of the section. For the steel the strains and therefore the stresses can readily be established. In the literature the compressive stress diagram for the concrete is generally characterised by two

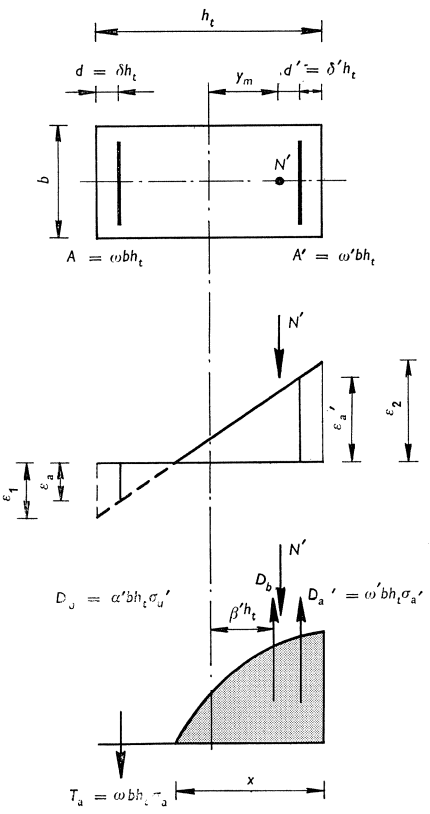

Fig. 2. Strains and forces associated with eccentric load on a rectangular section.

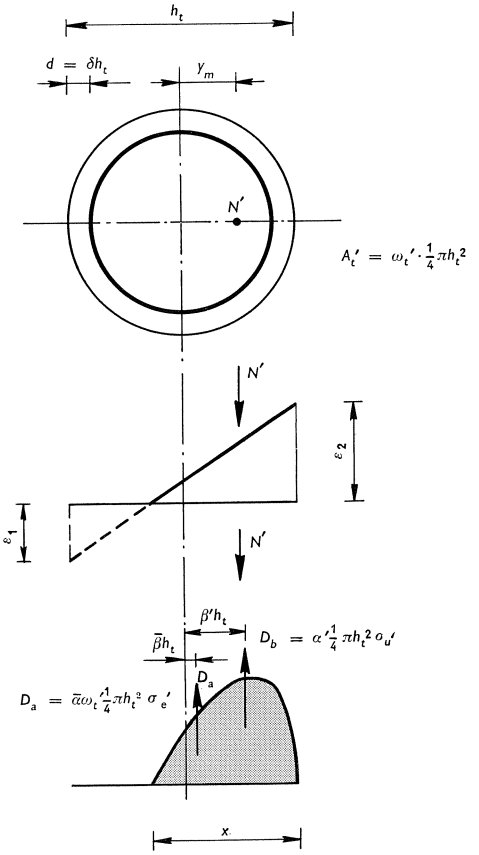

Fig. 3. Strains and forces associated with eccentric load on a circular section.

parameters α and β. The volume of the diagram thus becomes $D_b = \alpha b x \sigma_u'$, the distance of the resultant from the extreme compressive fibre being $y = \beta h_t$.

In connection with the following derivations these parameters have been modified to:

$$\alpha' = \alpha \frac{x}{h_t} \qquad \text{and}$$

$$\beta' = 0.5 - \beta$$

From the conditions $\Sigma N = 0$ and $\Sigma M = 0$ the following equations are obtained (positive algebraic signs denote compression):

$\Sigma N = 0 \quad N' = \alpha' \sigma_u' \, bh_t + \sigma_a' \omega' \, bh_t + \sigma_a \omega \, bh_t$ [1])

or
$$\frac{N'}{\sigma_u' \, bh_t} = \alpha' + \sigma_a' \frac{\omega'}{\sigma_u'} + \sigma_a \frac{\omega}{\sigma_u'} \quad \ldots \ldots \ldots \ldots \ldots \ldots \quad (1)$$

$\Sigma M = 0 \quad M = N' \cdot y_m = \alpha' \sigma_u' \, bh_t \cdot \beta' h_t + \sigma_a' \omega' \, bh_t (\tfrac{1}{2} - \delta) h_t - \sigma_a \omega b h_t (\tfrac{1}{2} - \delta) h_t$

or
$$\frac{M}{\sigma_u' \, bh_t^2} = \frac{N'}{\sigma_u' \, bh_t} \cdot \frac{y_m}{h_t} = \alpha' \beta' + \sigma_a' \frac{\omega'}{\sigma_u'} (\tfrac{1}{2} - \delta) - \sigma_a \frac{\omega}{\sigma_u'} (\tfrac{1}{2} - \delta) \ldots \quad (2)$$

On dividing equation (2) by $(1/2 - \delta)$ and on adding the equation thus obtained to, or on subtracting it from, equation (1), we obtain:

$$\frac{N'}{\sigma_u' \, bh_t} \left[1 + \frac{\frac{y_m}{h_t}}{\frac{1}{2} - \delta} \right] = \alpha' + \frac{\alpha' \beta'}{\frac{1}{2} - \delta} + 2\sigma_a' \frac{\omega'}{\sigma_u'} \quad \ldots \ldots \ldots \quad (3)$$

$$\frac{N'}{\sigma_u' \, bh_t} \left[1 - \frac{\frac{y_m}{h_t}}{\frac{1}{2} - \delta} \right] = \alpha' - \frac{\alpha' \beta'}{\frac{1}{2} - \delta} + 2\sigma_a \frac{\omega}{\sigma_u'} \quad \ldots \ldots \ldots \quad (4)$$

Similar conditions can be established for a member of circular cross-sectional shape. In the case of symmetrical reinforcement the latter can be conceived as an equivalent thin-walled cylinder having the same cross-sectional area (see Fig. 3). Then:

$\Sigma N = 0 \quad N' = \alpha' \cdot \frac{1}{4} \pi h_t^2 \sigma_u' + \bar{\alpha} \sigma_e' \omega_t' \cdot \frac{1}{4} \pi h_t^2$

where $\omega_t' = \dfrac{A_t'}{\frac{1}{4} \pi h_t^2}$ and A_t' = total reinforcement

or
$$\frac{N'}{\frac{1}{4} \pi h_t^2 \cdot \sigma_u'} = \alpha' + \bar{\alpha} \sigma_e' \frac{\omega_t'}{\sigma_u'} \quad \ldots \ldots \ldots \ldots \ldots \ldots \quad (1')$$

$\Sigma M = 0 \quad M = N' y_m = \alpha' \cdot \frac{1}{4} \pi h_t^2 \cdot \beta' h_t \cdot \sigma_u' + \bar{\alpha} \sigma_e' \cdot \bar{\beta} h_t \cdot \omega_t' \cdot \frac{1}{4} \pi h_t^2$

or
$$\frac{N'}{\frac{1}{4} \pi h_t^2 \cdot \sigma_u'} \cdot \frac{y_m}{h_t} = \alpha' \beta' + \bar{\alpha} \bar{\beta} \sigma_e' \frac{\omega_t'}{\sigma_u'} \quad \ldots \ldots \ldots \ldots \ldots \quad (2')$$

[1]) Where necessary, the notation of G.B.V. 1962 has been adhered to, except that $\omega = A/bh_t$ and not $\omega = 100A/bh_t\%$ as in G.B.V. 1962.

These states of stress arise in a structural member loaded by a direct force (longitudinal force) N' with a certain initial eccentricity e_0 which is provisionally assumed to be constant over the entire length of the member.

As already stated, the deflection due to this loading is assumed to be sinusoidal in shape. Taking the deflection at the centre ($x = 0$) as being $y = f$, we obtain the general expression for the deflection:

$$y = y_m \cos\frac{\pi x}{L} = (e_0+f)\cos\frac{\pi x}{L}$$

For $x = \frac{1}{2}l_c$ we have $y = e_0$, so that:

$$e_0 = y_m \cos\frac{\pi\vartheta}{2} = (e_0+f)\cos\frac{\pi\vartheta}{2} = (e_0+f)\Theta$$

where $\vartheta = \dfrac{l_c}{L}$ and $\cos\dfrac{\pi\vartheta}{2} = \Theta$.

Hence it also follows that:

$$f = e_0\left(\frac{1-\cos\frac{\pi\vartheta}{2}}{\cos\frac{\pi\vartheta}{2}}\right) = e_0\left(\frac{1-\Theta}{\Theta}\right) \quad . \quad . \quad (5)$$

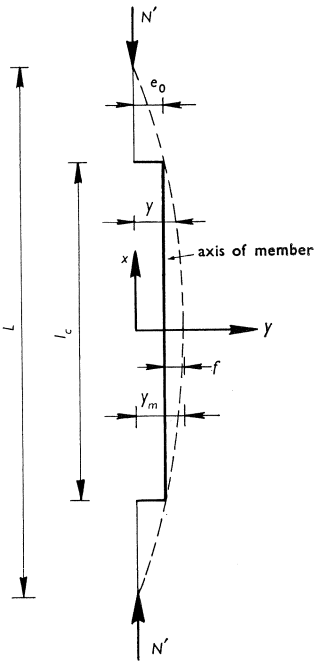

Fig. 4. Deflection of an eccentrically loaded member with a constant initial eccentricity e_0 along the axis of the member.

It can be shown that:

$$\frac{d^2y}{dx^2} = -y_m\frac{\pi^2}{L^2}\cos\frac{\pi x}{L}$$

and for $x = 0$ (critical section):

$$\frac{d^2y}{dx^2} = -y_m\frac{\pi^2}{L^2} = -(e_0+f)\left(\frac{\pi\vartheta}{l_c}\right)^2 \quad . \quad . \quad (6)$$

If furthermore:

$$\frac{1}{\varrho} = \frac{d^2y}{dx^2} = -\frac{\varepsilon_1-\varepsilon_2}{h_t} \quad . \quad . \quad . \quad . \quad . \quad . \quad . \quad (7)$$

(for $x = 0$ the values of ε_1 and ε_2 should be those associated with that particular section), then it follows from equations (6) and (7) that:

$$\frac{y_m}{h_t} = \frac{e_0+f}{h_t} = \frac{(\varepsilon_1-\varepsilon_2)\lambda^2}{\pi^2\vartheta^2} \quad . \quad . \quad . \quad . \quad . \quad . \quad . \quad . \quad . \quad . \quad . \quad . \quad . \quad (8)$$

where $\lambda = l_c/h_t$.

On substituting equation (5) into equation (8) we obtain:

$$\frac{f}{h_t} = \frac{(\varepsilon_1-\varepsilon_2)\lambda^2}{\frac{\pi^2\vartheta^2}{1-\Theta}} = \frac{(\varepsilon_1-\varepsilon_2)\lambda^2}{\Phi}$$

while:

$$\frac{e_0}{h_t} = \frac{(\varepsilon_1-\varepsilon_2)\lambda^2}{\Phi} \cdot \frac{\Theta}{1-\Theta} = \frac{(\varepsilon_1-\varepsilon_2)\lambda^2}{\frac{\pi^2\vartheta^2}{\Theta}} = \frac{(\varepsilon_1-\varepsilon_2)\lambda^2}{\Xi} \quad \ldots\ldots\ldots \quad (9)$$

Equation (8) can, finally, be written as follows:

$$\frac{y_m}{h_t} = \frac{e_0+f}{h_t} = \left(\frac{1}{\Xi}+\frac{1}{\Phi}\right)(\varepsilon_1-\varepsilon_2)\lambda^2 \quad \ldots\ldots\ldots\ldots\ldots \quad (8a)$$

where: $\dfrac{1}{\Xi}+\dfrac{1}{\Phi} = \dfrac{1}{\pi^2\vartheta^2}$.

The quantities Θ, Ξ and Φ are functions of $\vartheta = l_c/L$ only. From Table I it appears that for $\vartheta = 1.0$, *i.e.*, $l_c = L$, the value of $\Xi \to \infty$ and therefore $e_0 \to 0$. Associated with this is a value $\Phi = \pi^2$, so that we have for the deflection:

$$\frac{y_m}{h_t} = \frac{f}{h_t} = \frac{(\varepsilon_1-\varepsilon_2)\lambda^2}{\pi^2} \quad \ldots\ldots\ldots\ldots\ldots\ldots \quad (10a)$$

For $\vartheta \to 0$, and therefore $l_c \ll L$, we have $\Xi \to 0$ and consequently $e_0 \to \infty$. Hence this approaches the case of pure bending without direct force, and in this case we obtain for the deflection:

$$\frac{f}{h_t} \to \frac{(\varepsilon_1-\varepsilon_2)\lambda^2}{8} \quad \text{since } \Phi \to 8.0 \quad \ldots\ldots\ldots\ldots \quad (10b)$$

Table I

$\vartheta = \dfrac{l_c}{L}$	Θ	Ξ	Φ	$\dfrac{1}{\Xi}+\dfrac{1}{\Phi}$
1.0	0	∞	9.87($=\pi^2$)	0.1015
0.9	0.156	51.0	9.49	0.1251
0.85	0.234	30.5	9.30	0.1406
0.8	0.309	20.4	9.14	0.1585
0.7	0.454	10.64	8.85	0.2070
0.6	0.588	6.05	8.62	0.2815
0.5	0.707	3.48	8.42	0.406
0.4	0.809	1.95	8.26	0.635
0.3	0.891	1.00	8.15	1.123
0	1.000	0	8.00	∞

This deflection corresponds to that which occurs in a member loaded over its entire length (l) by a constant bending moment (M), since:

$$\frac{f}{h_t} = \frac{Ml^2}{8EI\,h_t} = -\frac{\mathrm{d}^2y}{\mathrm{d}x^2} \cdot \frac{l^2}{8h_t} = \frac{(\varepsilon_1-\varepsilon_2)}{8}\left(\frac{l}{h_t}\right)^2$$

The value of y_m/h_t as given by equation (8) or (8a) should be substituted into the equilibrium conditions (3) and (4). The effect of slenderness is thereby taken into account, and we thus obtain:

$$\frac{N'}{\sigma_u' \, bh_t}\left[1 + \frac{(\varepsilon_1-\varepsilon_2)\lambda^2}{\pi^2\vartheta^2(\frac{1}{2}-\delta)}\right] = \alpha' + \frac{\alpha'\beta'}{\frac{1}{2}-\delta} + 2\sigma_a' \frac{\omega'}{\sigma_u'} \quad \ldots\ldots\ldots (3')$$

$$\frac{N'}{\sigma_u' \, bh_t}\left[1 - \frac{(\varepsilon_1-\varepsilon_2)\lambda^2}{\pi^2\vartheta^2(\frac{1}{2}-\delta)}\right] = \alpha' - \frac{\alpha'\beta'}{\frac{1}{2}-\delta} + 2\sigma_a \frac{\omega}{\sigma_u'} \quad \ldots\ldots\ldots (4')$$

If all the dimensions of a structural member are given (*i.e.*, ω, ω', b, h_t, l_c and d), and also e_0 and σ_u', then there remain four unknowns – N', ε_1, ε_2 and ϑ – in the equations (3'), (4') and (9). (Note that α', β', σ_a and σ_a' are dependent only on ε_1 and ε_2, while Ξ is solely a function of ϑ). When a given load N' is applied to the member, the associated values of ε_1, ε_2 and ϑ can therefore be calculated with the aid of these equations. Any other value of N' yields different values of ε_1, ε_2 and ϑ. The relation between N', ε_1 and ε_2 is indicated diagrammatically in Fig. 5a.

1.1.3 Ultimate load

As appears from Fig. 5a, it is, above a certain maximum value N_{br}', no longer possible to satisfy the equilibrium conditions. Hence the value N_{br}' obviously represents the ultimate compressive force, *i.e.*, the compressive force producing failure of the member. In many cases, especially for fairly high values of the slenderness ratio and of the initial eccentricity, the value of ε_2 will, at the instant when N_{br}' is reached, be smaller than the maximum compressive strain of the concrete $\varepsilon_u' = 3.5^0/_{00}$. For small values of λ and/or of e_0, however, ε_2 may indeed attain the value of ε_u'. An example of each alternative possibility is given in Fig. 5b and 5c. (The data on which these graphs are based have been obtained from model tests – see 1.2.1).

Hence there are two criteria for the ultimate compressive force. In the case where the maximum compressive strain of the concrete is attained, this is a strength criterion for the ultimate compressive force N_{br}'; in the alternative case it is necessary to apply an equilibrium criterion, which could be formulated by the conditions:

$$\frac{dN'}{d\varepsilon_1} = 0 \quad \text{or} \quad \frac{dN'}{d\varepsilon_2} = 0, \quad \text{or, alternatively} \quad \frac{dN'}{d(\varepsilon_1-\varepsilon_2)} = 0 \quad \ldots (11)$$

Equation (11), in conjunction with equations (3'), (4') and (9), would then be sufficient for determining N_{br}' (four equations with four unknowns). In practice, however, this method of solution is found to yield very awkward and almost insoluble equations. For this reason a different procedure was sought. The following approach was adopted: Consider a structural member with given dimensions (*i.e.*, ω, ω', b, h_t, l_c and d are known), while σ_u' is also given. In equations (3'), (4') and (9) there then remain five unknowns, namely,

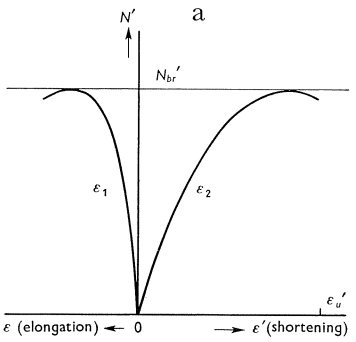

Fig. 5a. Diagrammatic representation of the relation between N', ε_1 and ε_2.

Fig. 5b. Relation between N', ε_1 and ε_2 as obtained from a model test (see 1.2.1) for a member of circular section ($h_t = 25$ cm; $l_c = 500$ cm; $l_c/h_t = 20$; QR(n) 40; $\omega_t'/\sigma_u' = 1 \times 10^{-4}$ cm²/kg; $e_0 = 5$ cm; $d = 3.75$ cm).

Fig. 5c. Relation between N', ε_1 and ε_2 as obtained from a model test (see 1.2.1) for a member of rectangular section ($h_t = 30$ cm; $l_c = 900$ cm; $l_c/h_t = 30$; QR(n) 40; $\omega/\sigma_u' = \omega'/\sigma_u' = 0.5 \times 10^{-4}$ cm²/kg; $e_0 = 6$ cm; $d = 3$ cm).

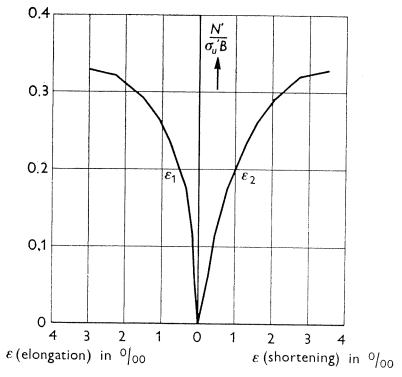

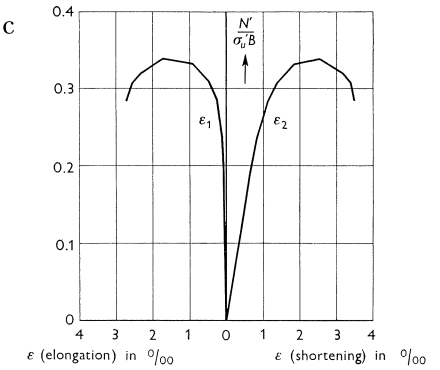

N', ε_1, ε_2, ϑ and e_0. Next, we start from a number of systematically chosen states of strain. Each state of strain is determined by a value of ε_2 (compressive strain), chosen between $3.5^0/_{00}$ (max. compressive strain of the concrete) and $0.25^0/_{00}$. Furthermore, for each value of ε_2 the value of ε_1 is varied from $3.5^0/_{00}$ (max. compressive strain) to – in some cases – an elongation of $30^0/_{00}$. In this way, therefore, the entire range of possible states of stress is covered. For an assumed state of strain the values of $N'/\sigma_u' \, bh_t$ and ϑ can be determined from the equations (3') and (4'). Thus the value of Ξ (Table I) is known and then e_0/h_t can be calculated from equation (9). Because of the arbitrary assumption as to the state of strain, the value found for N' will, generally speaking, not constitute a maximum associated with the value found for e_0. However, the relation between N' and e_0 can, for any particular value of ε_2, be plotted in a graph. In this way a number of lines can be drawn in a graph of this kind. It is found that all the lines together constitute an envelope which evidently indicates the relation between N_{br}' and e_0. This is shown diagrammatically in Fig. 6.

Thus the ultimate compressive force N_{br}' can be calculated as a function of the initial eccentricity e_0. The variables that have to be determined in advance are:

Fig. 6. Envelope formed by lines of constant value of ε_2 and indicating the relation between the ultimate load N_{br}' and the initial eccentricity e_0 for a member with given dimensions.

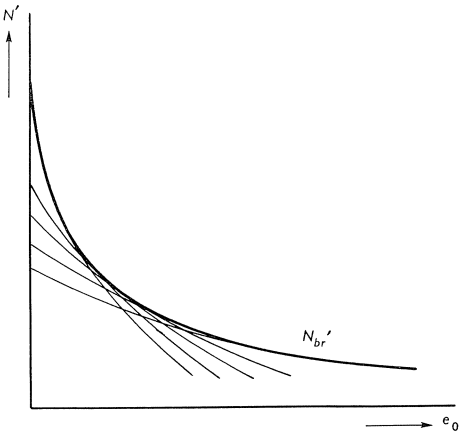

- cross-sectional shape (rectangular or circular);
- quality of steel (mild steel or high-tensile steel);
- percentage of reinforcement and distribution thereof over the compressive and the tensile sides of the section;
- concrete cover to the reinforcement;
- slenderness ratio $\lambda = l_c/h_t$.

As examples of the results so computed for a series of different values in 128 combinations of the above variables some diagrams are reproduced here (Figs. 7–12).

In the cases where $A \neq A'$ it is found that the maximum value of N_{br}' is reached for $e_0 \neq 0$. This will readily be understood in the case $\lambda = 0$. The highest attainable load on a structural member is the load at which the compressive strain has the value $\varepsilon_u' = 3.5^0/_{00}$ over the entire section. In that case $\alpha' = 1$ in equation (1), while $\sigma_a = \sigma_a' = \sigma_e'$, so that:

$$\frac{N_{br}'}{\sigma_u' \, bh_t} = 1 + \frac{\omega' + \omega}{\sigma_u'} \sigma_e'$$

Since $\beta' = 0$ in equation (2) (D_b acts centrally) and therefore $\alpha'\beta' = 0$, equation (2) becomes:

$$\frac{N_{br}'}{\sigma_u' \, bh_t} \cdot \frac{y_m}{h_t} = \frac{\omega' - \omega}{\sigma_u'} \sigma_e' \left(\tfrac{1}{2} - \delta\right)$$

In the case $\lambda = 0$ no deflection occurs, so that $y_m = e_0$ or:

$$\frac{N_{br}'}{\sigma_u' \, bh_t} \cdot \frac{e_0}{h_t} = \frac{\omega' - \omega}{\sigma_u'} \sigma_e' \left(\tfrac{1}{2} - \delta\right)$$

Note. In the case of non-constant eccentricity along the length of a member (see Fig. 13), the method of solution indicated in the foregoing can likewise

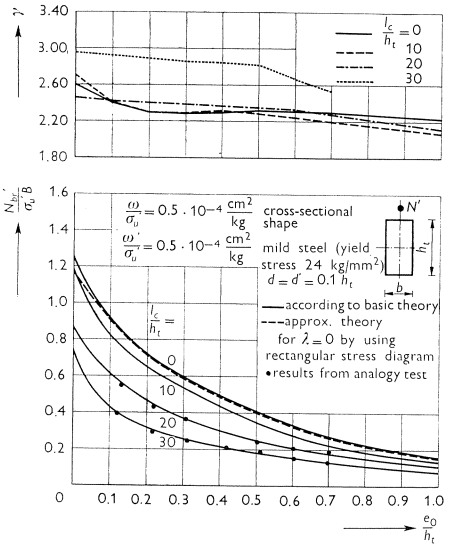

Fig. 7.

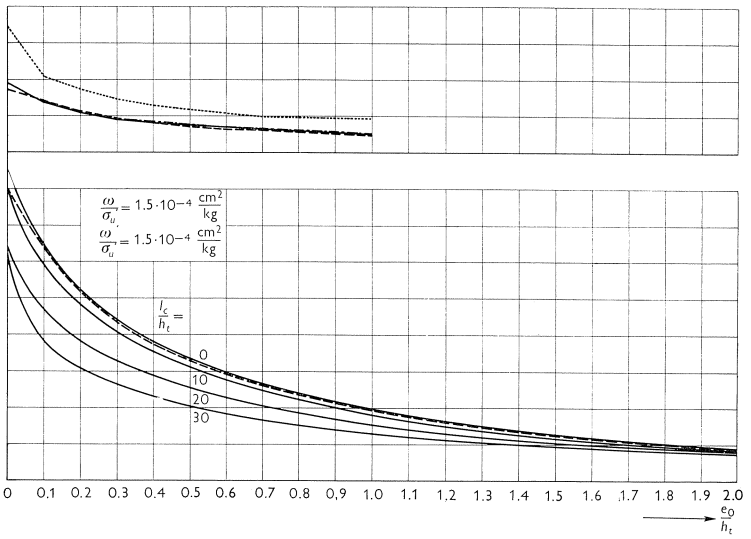

Fig. 8.

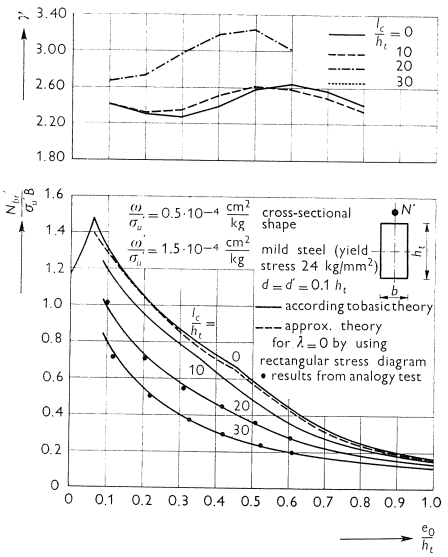

Fig. 9.

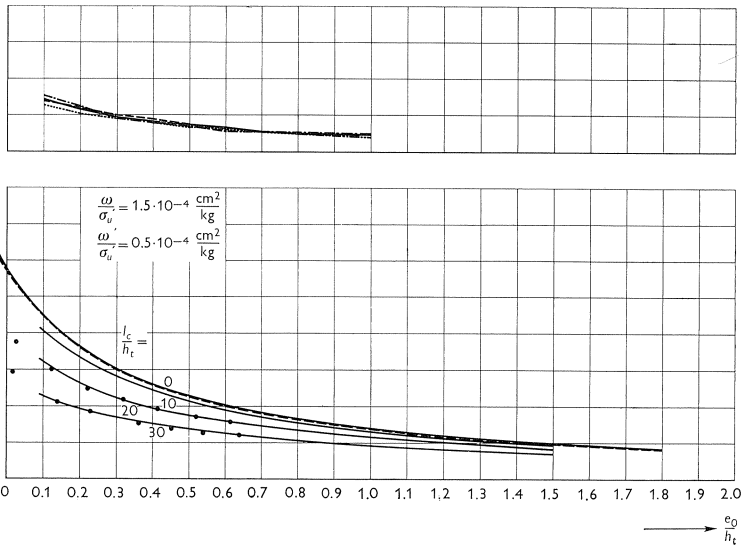

Fig. 10.

Fig. 7–12. Diagrams showing the ultimate load N_{br}' and the factor of safety γ against failure as functions of the initial eccentricity e_0. (For Fig. 11–12: p.t.o.).

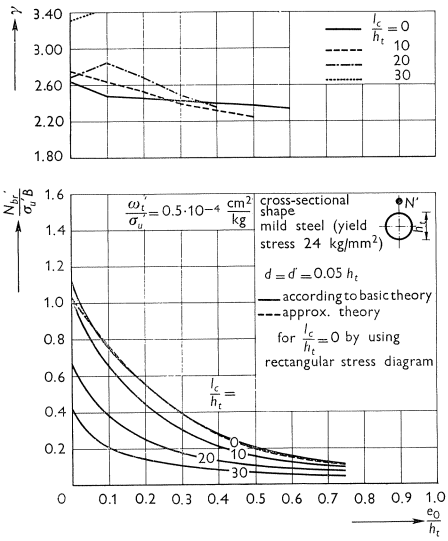

Fig. 11.

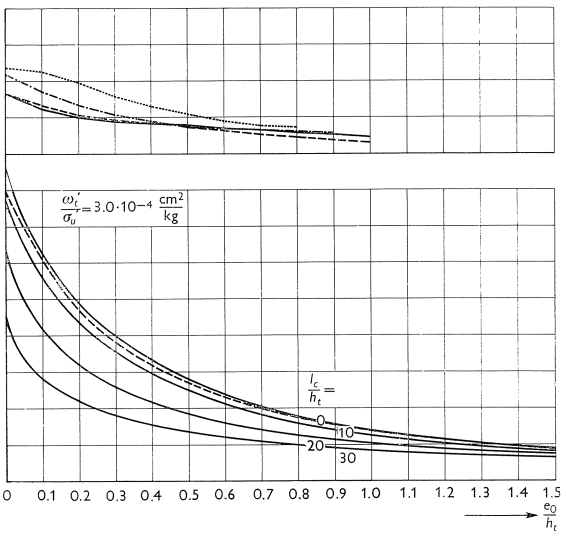

Fig. 12.

be used. Putting $e_w = \varkappa e_v$ (where it is assumed that $e_v \geqslant e_w$ and therefore $\varkappa \leqslant 1$), we can write:

$$e_v = y_m \cos \frac{\pi l_v}{L} = y_m \cos \pi\vartheta_v \quad . \quad . \quad . \quad (12)$$

where $l_v/L = \vartheta_v$

and $$e_w = \varkappa e_v = y_m \cos \frac{\pi l_w}{L} = y_m \cos \pi\vartheta_w \quad (13)$$

where $l_w/L = \vartheta_w$.

Hence it also follows that:

$$\vartheta_v + \vartheta_w = \frac{l_v + l_w}{L} = \frac{l_c}{L} = \vartheta.$$

From equations (12) and (13) can be derived:

$$\varkappa y_m \cos \pi\vartheta_v = y_m \cos \pi\vartheta_w = y_m \cos \pi(\vartheta - \vartheta_v)$$

or $$\varkappa \cos \pi\vartheta_v = \cos \pi\vartheta \cos \pi\vartheta_v + \sin \pi\vartheta \sin \pi\vartheta_v$$

so that $$\tan \pi\vartheta_v = \frac{\varkappa - \cos \pi\vartheta}{\sin \pi\vartheta} \quad . \quad . \quad . \quad . \quad . \quad . \quad (14)$$

For an assumed state of strain, again characterized by ε_1 and ε_2, the values of N' and y_m can, for example, be solved from equations (3) and (4). The associated value of ϑ can be calculated with the

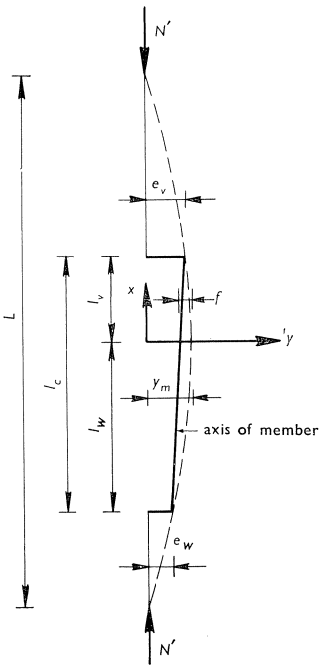

Fig. 13. Deflection of an eccentrically loaded member with eccentricity not constant along the axis of the member.

aid of equation (8). Hence, for a given value of $\varkappa$, the value of ϑ_v can be determined by means of equation (14), so that then ϑ_w is also known. The values of e_v and e_w are thereupon obtained from equations (12) and (13). We can now, in the manner already described, determine envelopes which give the relation between N_{br}' and, for example, e_v for a given value of $\varkappa$.

1.1.4 Effect of stress-strain diagram of concrete on ultimate load

In order to gain some idea of the effect of the stress-strain diagram of the concrete upon the ultimate load, the relation between N_{br}' and e_0 for $\lambda = 0$ has been calculated in a few cases, both with the diagram in Fig. 1b and with the diagram in Fig. 14. The latter could be taken as representing the stress-strain diagram for a test with loading of short duration, in which the scatter in the strength has not been taken into account (σ_u' = prism strength $\approx 0.85\ \sigma_{w_{28}}'$ – see 1.1.1). From Fig. 15 it appears that for small values of e_0 the difference is quite substantial, but that this difference becomes smaller – absolutely as well as relatively – with increasing values of e_0. We can take it that we shall be on the safe side with the stress-strain diagram represented in Fig. 1b.

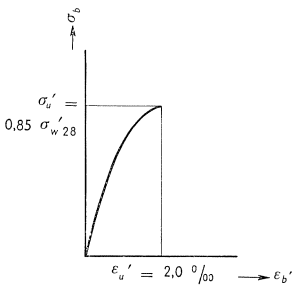

Fig. 14. Assumed stress-strain diagram.

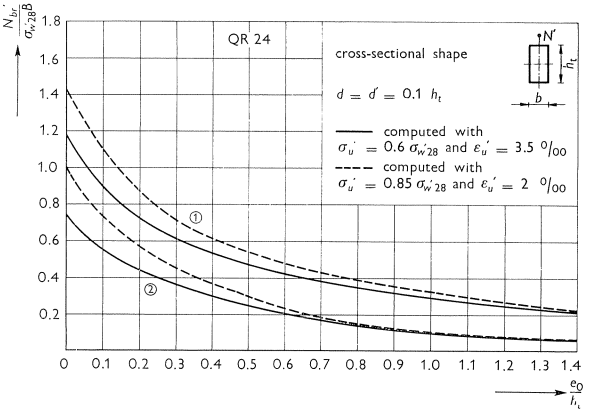

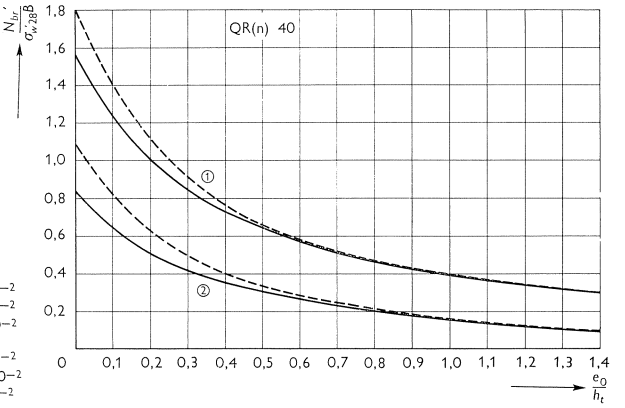

Fig. 15. Effect of the stress-strain diagram for concrete upon the ultimate load N_{br}' for $\lambda = 0$.

① $\omega = \omega' = 1{,}2 \cdot 10^{-4} \sigma_{w\,28}'$

K 160	$\omega = \omega' = 1{,}92 \cdot 10^{-2}$
K 225	$\omega = \omega' = 2{,}70 \cdot 10^{-2}$
K 300	$\omega = \omega' = 3{,}60 \cdot 10^{-2}$

② $\omega = \omega' = 0{,}3 \cdot 10^{-4} \sigma_{w\,28}'$

K 160	$\omega = \omega' = 0{,}48 \cdot 10^{-2}$
K 225	$\omega = \omega' = 0{,}675 \cdot 10^{-2}$
K 300	$\omega = \omega' = 0{,}90 \cdot 10^{-2}$

1.2 Experimental results

1.2.1 Model analogy

With a view to verifying the results of the calculations as represented in Figs. 7–31, a model analogy was used which is described in the preceding article in this issue. This model analogy is based on the same assumptions as those adopted in the calculations. The results of the model tests are indicated in various diagrams by means of dots. There is good agreement with the calculated values. The columns subjected to sustained loading tests by GAEDE – Report 129 of Deutscher Ausschuss für Stahlbeton – were thereupon analysed by means of the theory described in the foregoing and checked with the model analogy (see 1.2.2). Next, some T-section and trapezoidal section columns were analysed and also checked by means of model tests not described in this paper.

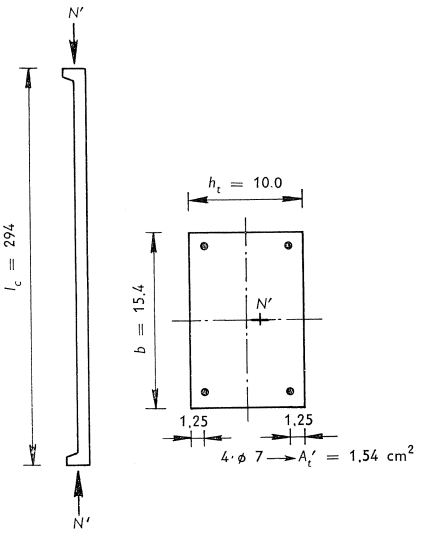

Fig. 16a. Columns tested by GAEDE (Report 129 D.A.f.S.) – dimensions in cm.

1.2.2 Tests by GAEDE and by the I.B.B.C.

As the theory described in this paper is based on various assumptions, it appeared expedient to check the results of that theory against test results obtained with structural members subjected to sustained loading. Unfortunately, there are only few investigations on record in which members with reasonable slenderness ratios [1]) were subjected to loading of this kind. Some data were obtained from the investigations described in the following.

GAEDE's tests were performed on columns as illustrated in Fig. 16a. The investigation comprised two series of tests, *viz.*, series I in which $e_0/h_t = 0.2$ and series II in which $e_0/h_t = 0.5$. Some data derived from the relevant report are indicated in Table II.

In Table III are given the results of the calculations according to the theory described here, and also the results of the model analogy. These results have, finally, been referred to those obtained by GAEDE.

---

[1]) J.A.C.I., March 1961, contains an article by I. M. VIEST, R. C. ELSTNER and E. HOGNESTAD, entitled: „Sustained load strength of eccentrically loaded short reinforced concrete columns". As the slenderness ratio was only about 8, the effect of this quantity on the ultimate load was, in our opinion, inadequately manifested in that investigation.

Table II. Data for columns tested under sustained loading by GAEDE.

column No.	$\frac{e_0}{h_t}$	$\lambda=\frac{l_c}{h_t}$	σ_e in kg/cm² tensile reinforcement	σ_e' in kg/cm² compress. reinforcement	σ'_{w28} in kg/cm²	N_{br}' in kg	$\frac{N_{br}'}{\sigma_u' b h_t}$	age at time of application of load, in days	age at failure, in days	duration of loading, in days
I-2	0.2	29.4	3635	3195	255	6330	0.268	28	45	17
I-3	0.2	29.4	3762	3210	278	6500	0.254	28	35	7
I-4	0.2	29.4	2898	2731	398	6820	0.186	28	129	101
I-6	0.2	29.4	3000	2965	394	8060	0.222	25	63	38
I-7	0.2	29.4	2856	2975	382	8150	0.231	28	$42^1/_2$	$14^1/_2$
II-1	0.5	29.4	3550	3115	269	2500	0.103	28	137	109
II-2	0.5	29.4	3385	3210	282	3250	0.125	28	566	538
II-3	0.5	29.4	3585	3210	254	3200	0.137	28	563	535

It appears that the results of the calculations are in very close agreement with those of the model tests. Discrepancies between the two sets of results may, for example, arise from inaccuracies in the dimensions of the model. Except in the case of column No. II-1 there is found to be fair agreement with GAEDE's results. Since column II-1 can, with regard to its material properties, be taken as equivalent to columns II-2 and II-3 (see Table II), while the method of loading was identical, the difference in behaviour between II-1, on the one hand, and II-2 and II-3, on the other, cannot be explained from the data published in Report 129 of the Deutscher Ausschuss für Stahlbeton.

The tests conducted by the I.B.B.C. were performed on columns constructed to reduced scale. The dimensions of these model columns are indicated in Fig. 16b. The slenderness ratio $\lambda = l_c/h_t$ was 27.7 and 37.7. The yield point of the steel was 3000 kg/cm², and the average 28-day cube strength of the concrete was 423 kg/cm² ($\sigma_u' = 254$ kg/cm²). The maximum load attained with

Table III. Comparison of $N_{br}'/\sigma_u' b h_t$.

column No.	$\frac{N_{br}'}{\sigma_u' b h_t}$ calculated (1)	$\frac{N_{br}'}{\sigma_u' b h_t}$ according to model (2)	$\frac{N_{br}'}{\sigma_u' b h_t}$ according to GAEDE (3)	$\frac{(1)}{(3)}$	$\frac{(2)}{(3)}$	duration of loading, in days
I-2	0.268	0.271	0.268	1.00	1.01	17
I-3	0.255	0.250	0.254	1.00^5	0.98^5	7
I-4	0.203	0.214	0.186	1.09	1.15	101
I-6	0.206	0.221	0.222	0.93	0.99^5	38
I-7	0.214	0.209	0.231	0.92^5	0.90^5	$14^1/_2$
II-1	0.149	0.148	0.103	1.44^5	1.43^5	109
II-2	0.142	0.134	0.125	1.13^5	1.07	538
II-3	0.155	0.150	0.137	1.13	1.09	535
average (except II-1)				1.03	1.03	
average (with II-1)				1.08	1.08	

sustained loading, for an initial eccentricity $e_0/h_t = 0.2$, was established with reference to a large number of test results. These are given in Table IV. In this case, too, there is seen to be reasonably good agreement between the calculated and the experimentally determined values.

Table IV. Comparison of $N_{br}'/\sigma_u' bh_t$.

$\lambda = \frac{l_c}{h_t}$	$\frac{N_{br}'}{\sigma_u' bh_t}$ calculated (1)	$\frac{N_{br}'}{\sigma_u' bh_t}$ measured (2)	$\frac{(1)}{(2)}$
27.7	0.264	0.274	0.96[5]
37.7	0.156	0.164	0.95
average			0.96

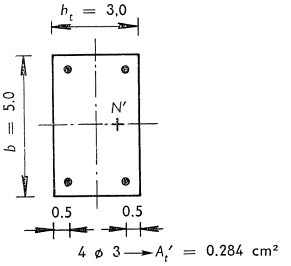

Fig. 16b. Columns to reduced model scale tested by the I.B.B.C. – dimensions in cm.

1.3 Ultimate load of an axially compressed member

For the analysis of an axially compressed structural member the ENGESSER-SHANLEY buckling theory, which makes use of the tangent modulus, was primarily applied. The tangent modulus associated with a stress σ is given by $E = d\sigma/d\varepsilon$ (see Fig. 17). If a material conforms to Hooke's Law, the value of E is independent of the magnitude of the stress. The ENGESSER-SHANLEY theory yields the lowest possible value of the buckling load.

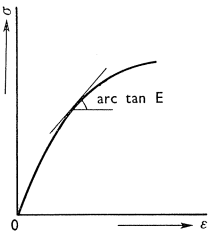

Fig. 17. Definition of tangent modulus.

For a member of rectangular cross-section, hinged at both ends, the following is true:

$$N_k' = \frac{\pi^2 EI}{l_c^2} \quad \ldots\ldots\ldots\ldots \quad (15)$$

where E denotes the tangent modulus. Furthermore:

$$N_k' = \sigma_b' \cdot bh_t + A_t' \sigma_a' \quad \ldots\ldots\ldots \quad (16)$$

where A_t' denotes the total amount of reinforcement, which is conceived as uniformly distributed along the sides b (Fig. 18). The quantities E, σ_b' and σ_a' are all functions of the strain ε' which, for axial loading, is of course constant over the entire cross-section. On equating (15) and (16) we obtain an equation in ε'. For a member with given dimensions the value of ε' can be calculated. The value of N_k' can then be determined.

In order to work out this procedure, we can, in the first place, transform (15) by substitution of the tangent modulus, which can be obtained from the stress-strain diagram.

The quadratic parabola in Fig. 1b, representing the stress-strain diagram of concrete, conforms to:

$$\sigma_b' = \sigma_u' \frac{\varepsilon'}{\varepsilon_u'}\left(2 - \frac{\varepsilon'}{\varepsilon_u'}\right) = \sigma_u'(2\eta - \eta^2)$$

where $\eta = \dfrac{\varepsilon'}{\varepsilon_u'}$.

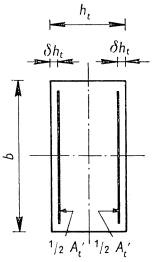

Fig. 18.

The tangent modulus can be determined from this, since:

$$E = \frac{d\sigma_b'}{d\varepsilon'} = \frac{2\sigma_u'}{\varepsilon_u'} - 2\sigma_u' \frac{\varepsilon'}{\varepsilon_u'^2} = 571.43\sigma_u'(1-\eta)$$

if $\varepsilon_u' = 3.5{}^0/_{00}$.

If no yielding of the steel occurs, we have for a member of rectangular section and containing a steel cross-sectional area $A_t' = \omega_t' b h_t$:

$$EI = \frac{571.43\sigma_u'(1-\eta)}{12} bh_t^3 + \omega_t' bh_t(0.5h_t - \delta h_t)^2 \cdot E_a'$$

where $E_a' = 2.1 \times 10^6$ kg/cm², so that:

$$EI = \sigma_u' bh_t^3 \left[47.619 - 47.619\eta + 2.1 \cdot 10^6 \frac{\omega_t'}{\sigma_u'}(0{,}5-\delta)^2\right] = \sigma_u' bh_t^3 \cdot K$$

Substitution of this value in equation (15) gives:

$$N_k' = \frac{\pi^2 \sigma_u' bh_t^3}{l_c^2} \cdot K \quad \text{or}$$

$$\frac{N_k'}{\sigma_u' bh_t} = \frac{9.8696}{\lambda^2} \cdot K \quad \ldots\ldots\ldots\ldots\ldots\ldots\ldots \quad (17)$$

where $\lambda = l_c/h_t$.

The summation of (16) formula can be written as follows:

$$N_k' = \sigma_u'(2\eta - \eta^2)\, bh_t + \omega_t' bh_t \varepsilon' E_a'$$

or, since $\varepsilon' = \eta \cdot \varepsilon_u' = \eta \cdot 3.5 \cdot 10^{-3}$:

$$\frac{N_k'}{\sigma_u' bh_t} = 2\eta - \eta^2 + 7350\eta \frac{\omega_t'}{\sigma_u'} \quad \ldots\ldots\ldots\ldots\ldots\ldots\ldots \quad (18)$$

On equating (17) and (18) we obtain:

$$\eta^2 - \eta\left(\frac{470}{\lambda^2} + 7350\frac{\omega_t'}{\sigma_u'} + 2\right) + \frac{2072.62 \cdot 10^4}{\lambda^2} \cdot \frac{\omega_t'}{\sigma_u'}(0.5-\delta)^2 + \frac{470}{\lambda^2} = 0 \quad \ldots \quad (19)$$

If ω_t', λ, δ and σ_u' are known, then η and therefore ε' can be determined from equation (19). With the aid of (17) or (18) we can also find N_k'. However, if the value of ε' obtained from (19) is found to be larger than ε_e' (see Fig. 1a), then the solution is incorrect because in that case yielding of the steel would

occur, so that $\sigma_a' = \sigma_e'$ and $E_a' = 0$. Equations (17) and (18) will then become, respectively:

$$\frac{N_k'}{\sigma_u' \, bh_t} = \frac{470}{\lambda^2}(1-\eta) \quad \ldots \ldots \ldots \ldots \ldots \ldots \ldots \ldots \quad (17a)$$

$$\frac{N_k'}{\sigma_u' \, bh_t} = 2\eta - \eta^2 + \sigma_e' \frac{\omega_t'}{\sigma_u'} \quad \ldots \ldots \ldots \ldots \ldots \ldots \ldots \quad (18a)$$

Fig. 19–22. Diagrams showing the ultimate load N_{br}' as a function of the slenderness ratio λ for $e_0 = 0$.

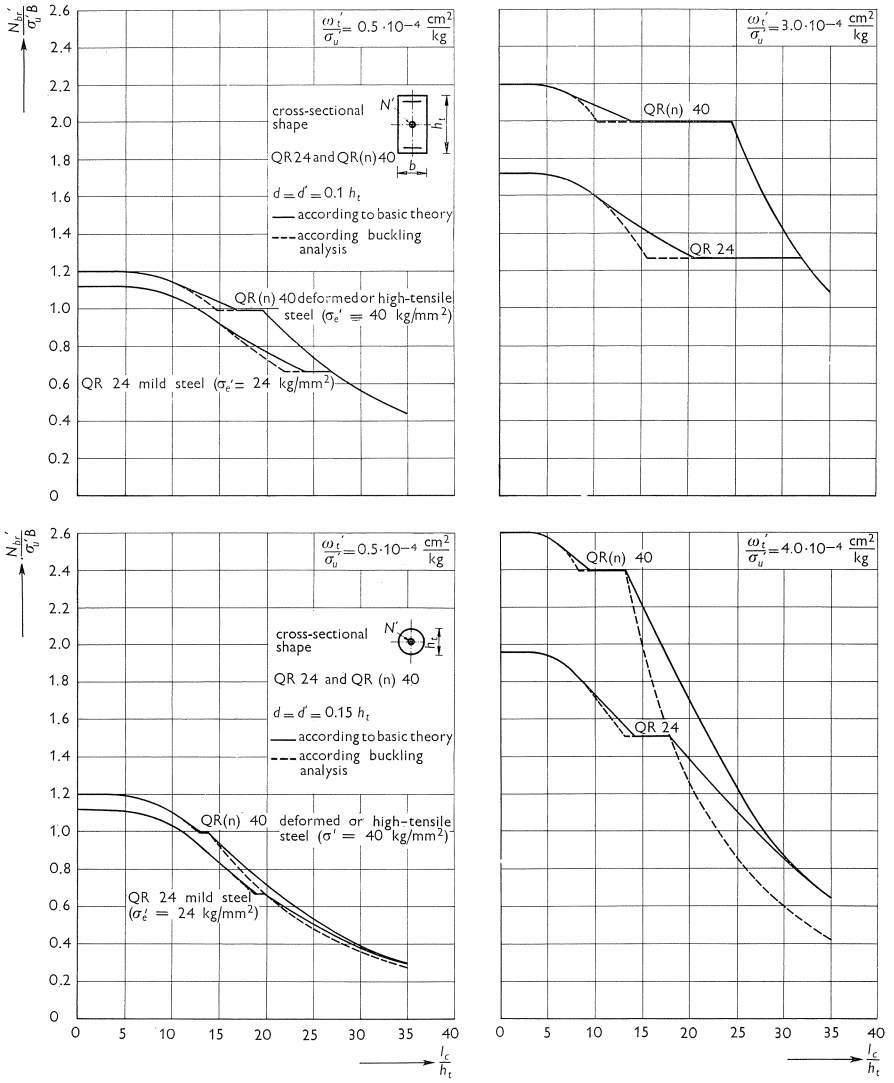

On equating these expressions, we obtain:

$$\eta^2 - \eta\left(\frac{470}{\lambda^2} + 2\right) - \sigma_e' \frac{\omega_t'}{\sigma_u'} + \frac{470}{\lambda^2} = 0 \quad \ldots\ldots\ldots\ldots \quad (19a)$$

Similar considerations are, of course, applicable to members of circular cross-section.

The relation between N_k' and λ was calculated for 13 combinations. Figs. 19–22 are given by way of example. It appears that each graph comprises three discontinuous portions. The curved portion on the left represents equation (19a). Then comes a horizontal portion which is longer in proportion as the steel percentage ω' is higher and which is connected to a second curved portion. The latter represents conditions in which the steel does not reach its yield point because the high slenderness ratio determines the load-carrying capacity of the member.

It is known that stable states of equilibrium $y_m \neq 0$ may still occur at loads in excess of the buckling loads calculated according to the ENGESSER-SHANLEY theory. Starting from the theory of eccentrically compressed structural members, the maximum values of these loads were calculated for $e_0 \to 0$. These loads have likewise been included in Figs. 19–22. In some cases, *e.g.*, with members of circular cross-section with a large quantity of reinforcement, these loads were found to be substantially larger than the calculated buckling loads; in other cases the buckling loads were found to constitute the maximum loads. The full lines in the above-mentioned diagrams represent these maximum loads (again designated by N_{br}') as functions of λ. In these diagrams the values of N_{br}' for, respectively, $\lambda = 0$, 10, 20 and 30, of course correspond, in similar cases, with those values which constitute the starting points ($e_0 = 0$) of the various λ-lines in Fig. 7–12.

1.4 Permissible load

1.4.1 Determining the additional eccentricities e_1 and e_2

With each value of the ultimate load N_{br}', as indicated in Figs. 7–12, is associated a certain state of strain determined by the values of ε_1 and ε_2. It appears that in the theoretically extreme case $\lambda = l_c/h_t = 0$ the ultimate load is always reached when $\varepsilon_2 = \varepsilon_u' = 3.5^0/_{00}$. Hence if, for a member with given dimensions, the value of $y_m = e_0$ (no deflection, since $\lambda = 0$) in equations (1) and (2) or (3) and (4) is assumed to be known, then there still remain two unknowns, *viz.*, ε_1 and the ultimate load N_{br}'. For $\lambda = 0$ the relation between N_{br}' and e_0 can therefore readily be determined. For other values of λ it often occurs that $\varepsilon_2 \neq \varepsilon_u'$ when the maximum load is reached, so that in these cases the envisaged relation is not so simple to calculate. However, by increasing the initial eccentricity e_0 in these cases by an additional eccentricity e_2 that is dependent on λ (see Fig. 23), it is nevertheless sufficient merely to carry out a

Fig. 23. Definition of the additional eccentricity e_2.

Fig. 24. Definition of the eccentricity e_1

$$\left[\frac{a}{b} = \frac{\gamma_{(e_0 = 0)}}{\gamma_{(e_0 = \infty)}} \approx \frac{2.5}{1.8}\right]$$

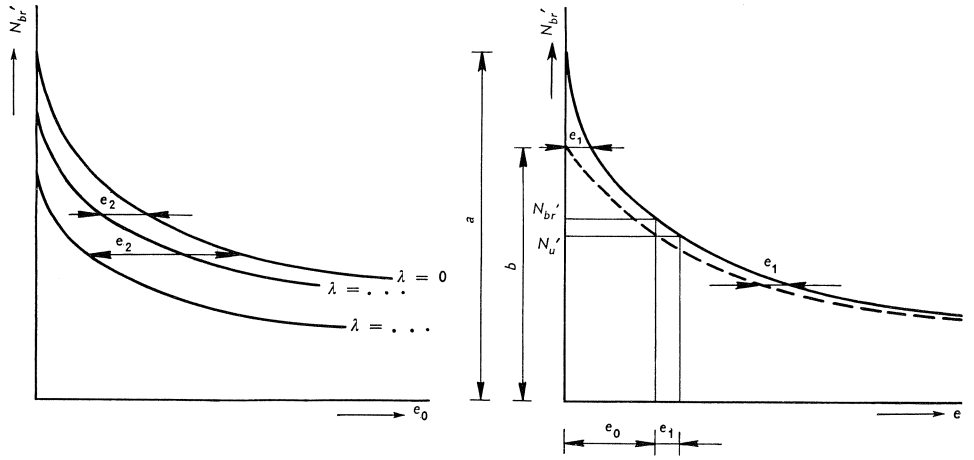

simplified calculation of the section ($\lambda = 0$ and $\varepsilon_2 = 3.5^0/_{00}$) in order to determine the correct value of N_{br}' associated with the given values of e_0 and λ.

To arrive at a permissible load, the ultimate load should be divided by a factor of safety (load factor) γ. It was considered necessary, in drawing up the regulations, to adopt in the case of axial compression ($e_0 = 0$) a higher value for this factor (approx. 2.5) than in the case of bending without direct force ($e_0 \rightarrow \infty$; $\gamma = 1.80$). For example, it is clearly apparent from Fig. 7 (et seq.) that a wrong estimation of the effective length (and therefore of λ) has a much greater effect upon N_{br}' for $e_0 = 0$ than it has for very large values of the eccentricity. In Fig. 15 a possible wrong estimation of the strength exhibits a similar tendency. It appeared to be desirable to provide a gradual transition of the value of γ for intermediate values of e_0. To achieve this, it is always possible, independently of the value of e_0, to make use of the value of γ for $e_0 \rightarrow \infty$ (viz., 1.80), provided that the initial eccentricity e_0 is increased by an additional amount e_1 (see Fig. 24). In this way a reduced ultimate load N_u' is obtained, which is therefore smaller than N_{br}'. The permissible load will then always be $\overline{N}' = N_u'/1.80$.

The values of e_1 and e_2 were determined from the results of all the cases analysed (see page 24). It has been endeavoured to keep the formulas for these quantities as simple as possible. To that end, in the case $e_0 = 0$, the safety factor has been somewhat reduced for large, and somewhat increased for small reinforcement amounts. This reduction or increase of the factor appeared justified, since in these cases the steel resists a large or a small proportion of the load respectively. The aim has been to obtain a value of the safety factor γ that would be reasonable in all cases, to ensure a gradual variation of this

factor with increasing value of e_0, and in general to provide somewhat larger values of γ for large values of λ. Having regard to these considerations, the value of e_2 was found to present a substantially linear relation with λ^2, more or less dependent on the steel quality (σ_e'), the cross-sectional shape (i), and the initial eccentricity e_0. The value of e_1 was, in the main, determined for the case $\lambda = 0$ and was found to be mainly dependent upon the cross-sectional shape (k). The two formulas are as follows:

$$e_1 = 0.78 k_1 \quad \ldots\ldots\ldots\ldots\ldots\ldots\ldots\ldots \quad (20)$$

where:

k_1 = the (larger) core radius in the direction of bending of the non-reinforced, uncracked section conceived as exhibiting linear elastic behaviour

$$(k_1 = W_{\max}/B)$$

and

$$e_2 = \left(0.85 + \frac{\sigma_e'}{16000}\right) \frac{0.23+6\dfrac{e_0}{h_t}}{\dfrac{i}{h_t}\left(0.22+3\dfrac{e_0}{h_t}\right)} \left(\frac{l_c}{100 h_t}\right)^2 h_t \quad \ldots\ldots\ldots \quad (21)$$

where:

i = the radius of gyration corresponding to the principal axis in the direction of bending of the non-reinforced, uncracked section conceived as exhibiting linear elastic behaviour

$$\left(i = \sqrt{\frac{I}{B}}\right).$$

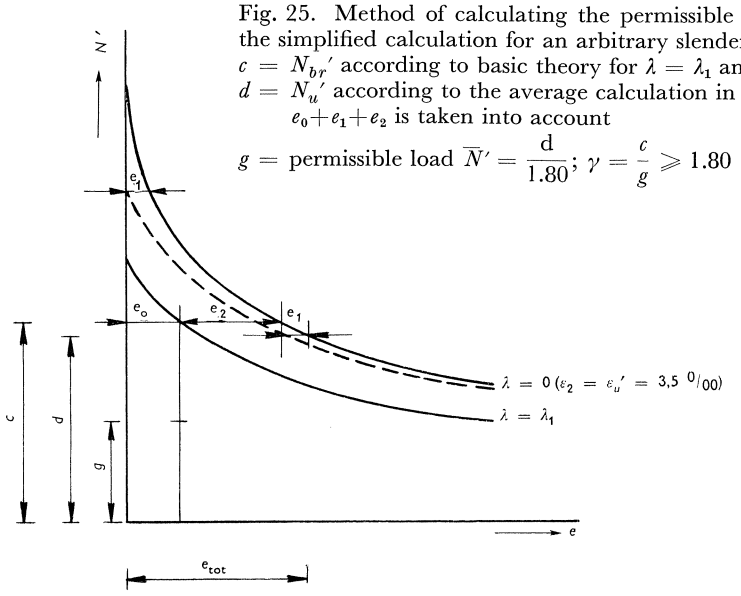

Fig. 25. Method of calculating the permissible load with the aid of the simplified calculation for an arbitrary slenderness ratio
$c = N_{br}'$ according to basic theory for $\lambda = \lambda_1$ and e_0
$d = N_u'$ according to the average calculation in which $e_{tot} = e_0+e_1+e_2$ is taken into account
g = permissible load $\overline{N}' = \dfrac{d}{1.80}$; $\gamma = \dfrac{c}{g} \geqslant 1.80$

Fig. 26. Behaviour and scatter of the safety factor γ as a function of e_0 for various values of λ.
a. $\lambda=0$; b. $\lambda=10$; c. $\lambda=20$; d. $\lambda=30$; e. average factor of safety (γ_{gem}).

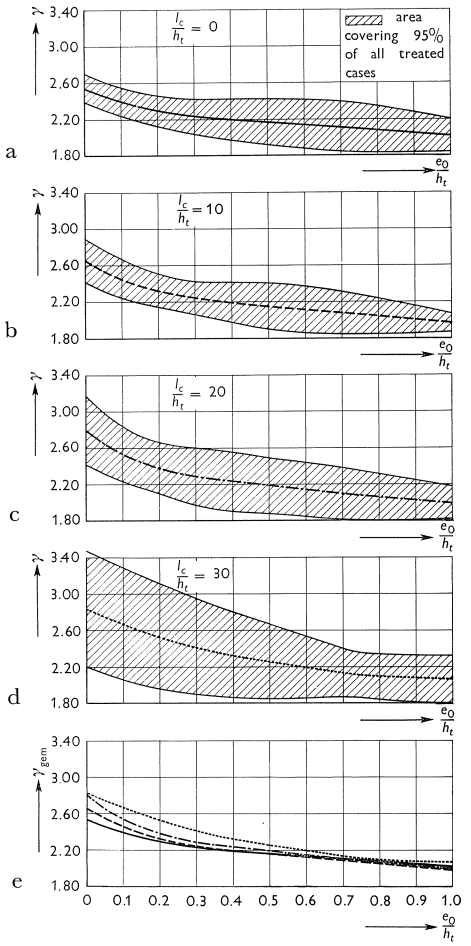

Fig. 25 gives a diagrammatic survey of the way in which the various eccentricities are taken into account and of the determination of γ. In Figs. 7–12 the behaviour of γ as a function of e_0 is indicated for the cases considered in those diagrams. For the cases with asymmetrical reinforcement the peaks of the λ-lines in these diagrams, as already stated, are not located on the vertical corresponding to $e_0 = 0$; for $\omega' > \omega$ they are – because of the asymmetry of the section – located at values of e_0/h_t which are a little larger than zero. In order to avoid undesirable (too low) values of γ in this region, the regulations stipulate that for an eccentricity $e_0/h_t < 0.1$ the member must always be symmetrically reinforced.

Table V. Factors of safety relating to columns tested by GAEDE and I.B.B.C.

column No.	$\frac{e_0}{h_t}$	$\lambda = \frac{l_c}{h_t}$	$\frac{\overline{N'}}{\sigma_u' b h_t}$	γ	load duration, in days
GAEDE					
I-2	0.2	29.4	0.100	2.68	17
I-3	0.2	29.4	0.095[5]	2.66	7
I-4	0.2	29.4	0.059	3.15	101
I-6	0.2	29.4	0.060	3.70	38
I-7	0.2	29.4	0.060	3.85	$14^1/_2$
II-1	0.5	29.4	0.059	1.75	109
II-2	0.5	29.4	0.053[5]	2.34	538
II-3	0.5	29.4	0.061[5]	2.23	535
I.B.B.C.	0.2	27.7	0.100	2.75	∞
I.B.B.C.	0.2	37.7	0.054	3.04	∞

In Fig. 26, for various values of γ, the average of γ has been plotted as a function of e_0/h_t for all the cases analysed by the I.B.B.C. The zone within which 95% of all the observations are located is also indicated. Table V gives the values of γ for GAEDE's columns and for those tested by the I.B.B.C. Starting from the data relating to the materials, the permissible loads were determined in the manner described above and were divided by the experimentally determined ultimate loads (see Tables II and IV). Except in the case of GAEDE's column II-1 the safety against failure is adequate in all cases. But even for this column II-1 there is still a fair margin of safety, viz. 1.75.

The important new feature to emerge from the foregoing considerations is that, for practical purposes, it is quite simply possible, by means of an additional eccentricity (e_1), to take account of a safety factor that varies with e_0. Secondly, the complex calculations that would have to be performed in the case where the equilibrium criterion (page 22) is decisive, can be reduced to a simpler analysis likewise by the introduction of an additional eccentricity (e_2). In the two equilibrium conditions (3) and (4) the quantity y_m should, in that case, be replaced by $e_{\text{tot}} = e_0+e_1+e_2$. For complete attainment of the maximum compressive strain of the concrete at the most highly compressed fibre ($\varepsilon_2 = \varepsilon_u' = 3.5{}^0/_{00}$) the ultimate load N_u' can then be calculated from the set of equations:

$$\frac{N_u'}{\sigma_u' \, bh_t}\left[1+\frac{\frac{e_{\text{tot}}}{h_t}}{\frac{1}{2}-\delta}\right] = \alpha' + \frac{\alpha'\beta'}{\frac{1}{2}-\delta} + 2\sigma_a' \frac{\omega'}{\sigma_u'} \quad \ldots\ldots\ldots \quad (3'')$$

$$\frac{N_u'}{\sigma_u' \, bh_t}\left[1-\frac{\frac{e_{\text{tot}}}{h_t}}{\frac{1}{2}-\delta}\right] = \alpha' - \frac{\alpha'\beta'}{\frac{1}{2}-\delta} + 2\sigma_a \frac{\omega}{\sigma_u'} \quad \ldots\ldots\ldots \quad (4'')$$

Starting from equations (1') and (2') we thus obtain for members of circular cross-sectional shape:

$$\frac{N_u'}{\sigma_u' \frac{1}{4}\pi h_t^2} = \alpha' + \bar{\alpha}\sigma_e' \frac{\omega_t'}{\sigma_u'} \quad \ldots\ldots\ldots\ldots\ldots\ldots \quad (1'')$$

$$\frac{N_u'}{\sigma_u' \frac{1}{4}\pi h_t^2} \cdot \frac{e_{\text{tot}}}{h_t} = \alpha'\beta' + \bar{\alpha}\bar{\beta}\sigma_e' \frac{\omega_t'}{\sigma_u'} \quad \ldots\ldots\ldots\ldots\ldots\ldots \quad (2'')$$

The factor of safety (load factor) to be taken into account is 1.80 in all cases.

The method of analysis described in the foregoing is, of course, suitable for the compilation of tables and graphs in a fashion similar to that applied in the conventional method. Indeed, there is a good deal of similarity between the two methods in so far as the calculation for determining the cross-section of the member is concerned. The load-factor method, as distinct from the conventional method, however, makes use of a parabolic stress-strain diagram for concrete; on the other hand, the steel stresses are, generally speaking, easier to determine since the yield stress is often reached.

1.4.2 Procedure of the calculation

Design calculation. Given a structural member of rectangular cross-section with dimensions b and h_t. Further known data are the design load $\bar{N}'$, the initial eccentricity e_0, the slenderness ratio $\lambda = l_c/h_t$, the concrete cover d, and the concrete and steel qualities. Determine ω and ω'.

We assume a state of strain for which $\varepsilon_2 = \varepsilon_u' = 3.5^0/_{00}$ and which is furthermore determined by $x = x_1$ (see Fig. 27). Since $N_u' = 1.80\ \bar{N}'$ and $e_{tot} = e_0 + e_1 + e_2$, there remain the unknowns ω and ω' in the equations (3'') and (4''). These unknowns can now therefore be solved, or they may be obtained from an appropriate graph. For each value of x we find an associated pair of values of ω and ω'. Hence there is an infinite number of solutions. A unique solution will be obtained only if we impose an additional condition, *e.g.*, $\omega = \omega'$ or $\omega + \omega' =$ minimum (see Fig. 28).

Fig. 28. ω and ω' as functions of x.

Fig. 27.

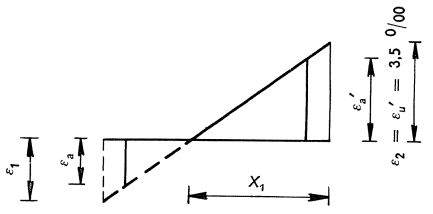

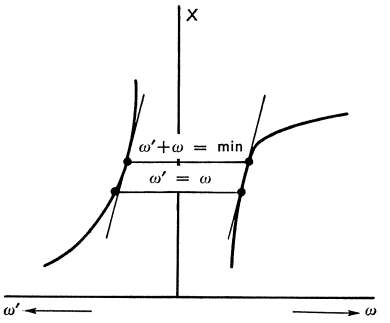

Check calculation. Given all the dimensions of the structural member, the initial eccentricity e_0, and the concrete and steel qualities. Determine the permissible load $\bar{N}'$.

The magnitude of $e_{tot} = e_0 + e_1 + e_2$ is known; the position of $N_u' = 1.80\ \bar{N}'$ is therefore given. We shall again assume a state of strain determined by $\varepsilon_2 = \varepsilon_u' = 3.5^0/_{00}$ and $x = x_1$. All the internal forces and their positions are then known. Now we determine N_u' and M_u in relation to the centroid of the section. Then $M_u/N_u' = e$. Since x has been arbitrarily chosen, in general: $e \neq e_{tot}$. By varying x, however, we find various associated values of e. The correct value of x can, for example, be obtained in the manner indicated diagrammatically in Fig. 29. The value of N_u' associated with $\bar{x}$ gives the permissible load $\bar{N}' = N_u'/1.80$. There is only one solution.

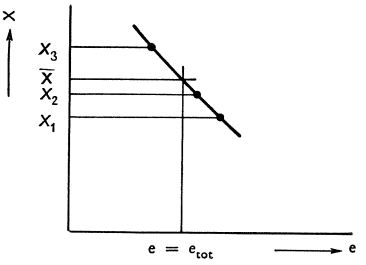

Fig. 29. Determination of N_u' for check calculation.

2 Approximations

Clause 48 of G.B.V. 1962 gives some approximate methods which aim at reducing the amount of arithmetical work and/or making complex cross-sectional shapes more amenable to analysis. As these approximations also occur in foreign literature on the subject of failure, it would appear appropriate to discuss briefly their arrangement and purport. In general, these procedures will involve the use of somewhat larger quantities of materials than does the design method set forth in 1.4.1.

2.1 Rectangular stress-strain diagram for concrete

Instead of adopting a parabolic stress-strain diagram for concrete, as in Fig. 1b, we may base ourselves upon the simplified diagram in Fig. 30. We shall consider the consequences of this simplified assumption in the case of a rectangular cross-section of a structural member. In order to obtain the same value for the magnitude of D_b in both cases, the following relation must exist between x_r (rectangular diagram) and x_p (parabolic diagram) (see Fig. 31):

$$x_r = \tfrac{2}{3}x_p$$

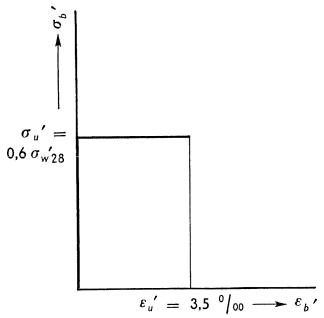

Fig. 30. Simplified stress-strain diagram for concrete.

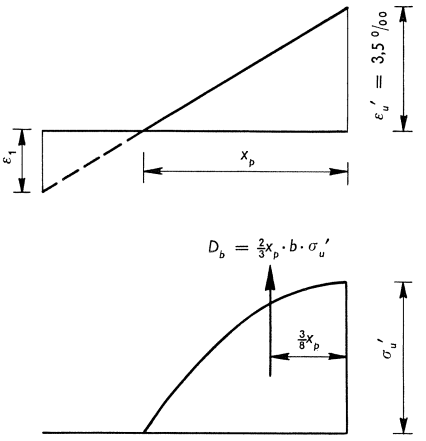

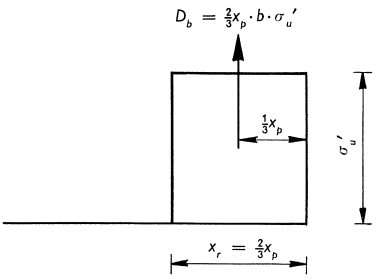

Fig. 31. Approximation of a parabolic compressive stress diagram by a rectangular diagram.

For a rectangular diagram the distance from D_b to the centroid of the section is somewhat in excess, however, and so the contribution of D_b to the internal moment is also somewhat greater.

Conversely, for determining the forces in the steel, the value of x_r must be increased by 50% in order to obtain the value of x_p. The state of strain is determined by x_p and $\varepsilon_2 = \varepsilon_u' = 3.5‰$, and hence the steel stresses are also determined.

The internal moment calculated on the assumption of a rectangular stress diagram is therefore too large, whereas the direct force has the correct value. The associated eccentricity of the direct force is therefore also too large. This could quite simply be corrected by increasing the eccentricity of the external load. As a result of introducing this additional eccentricity, the calculation is performed with an eccentricity that is so increased that the correct value of the ultimate load or the load that the member is able to carry (as the case may be) is nevertheless obtained.

In the case of bending without direct force the introduction of a rectangular stress diagram likewise yields too high a value of the ultimate moment. In that case, however, in order to obtain nevertheless the correct value of the permissible moment, it is simpler to divide the ultimate moment by a somewhat larger factor of safety. For this reason, the value of the factor of safety has been increased from 1.80 to 1.85 in Clause 48.

To obtain a gradual transition to large values of e_0 for bending in combination with direct force, the increased value of γ has been retained in this case. Besides, it was found to be necessary, more particularly for small values of e_0, to introduce an additional eccentricity e_3. The following expression for the value of e_3 was determined from all the 128 cases analysed:

$$e_3 = 0.003 \frac{h_t^2}{k_2} \quad \ldots\ldots\ldots\ldots\ldots\ldots\ldots\ldots\ldots \quad (22)$$

where k_2 denotes the (smaller) core radius in the direction of bending of the non-reinforced, uncracked section conceived as exhibiting elastic behaviour.

The results of the calculations for $\lambda = 0$ are indicated by broken lines in the relevant diagrams (Fig. 7–12).

To summarise, it can be stated that, if a rectangular stress diagram is adopted, the total eccentricity is:

$$e_{tot} = e_0 + e_1 + e_2 + e_3$$

while the factor of safety (load factor) is 1.85.